

Monitoring of forest fires from space – ISRO’s initiative for near real-time monitoring of the recent forest fires in Uttarakhand, India

Forest fire or wild land fire causes adverse ecological, economic and social effects worldwide^{1,2}. Globally, forest fires are considered as one of the major drivers of climate change having deleterious impacts on the earth and environment as studies reveal their significance in producing large amounts of trace gases and aerosol particles, which play a pivotal role in tropospheric chemistry and climate^{3–5}. Fire is an ecological process that has affected and shaped terrestrial systems and plant communities. Fire resets vegetation successional trajectories, sets up and maintains a dynamic mosaic of different vegetation structures and compositions, and reduces fuel accumulation. Human action disrupts these processes, with consequential fire behaviour and effects outside the range of natural variation⁶.

About 55% of the forest cover is subjected to fires each year, causing an economic loss of over 440 crores of rupees apart from other ecological effects⁷. The Forest Survey of India (FSI) has estimated that 1.45 m ha of forest is affected by fire annually with 6.17% of the forests prone to severe fire damage⁸. Satellite observations have been the only source of observations on fires on a global scale. Hotspots have been observed from a variety of sensors like AVHRR⁹, ATSR¹⁰, TRMM VIRS¹¹, MODIS¹², and the geostationary satellites GOES¹³ and MSG¹⁴.

Active forest fire monitoring using satellite data has been carried out from 2006 as part of the Disaster Management Support Programme of ISRO. The activity provides timely information on fires to State Forest Departments across India for forest fire control and management activities. Active fire monitoring uses satellite data from MODIS flying on the TERRA and AQUA spacecraft and Visible Infrared Imaging Radiometer Suite data from the Suomi National Polar-orbiting Partnership (SNPP-VIIRS). Satellite data are received and processed at Shadnagar, Telangana in near real-time using science process algorithms (SPAs) obtained from the Direct Readout Portal (<https://directreadout.sci.gsfc.nasa.gov>). The algorithms used are described in the literature^{15–17}. Information regarding active forest fire location is disseminated

to FSI and State Forest Departments through e-mail and short message service (SMS) within half an hour of satellite overpass. The information is also published in BHUVAN (<http://bhuvan.nrsc.gov.in/disaster/disaster/disaster.php?id=fire>). Post-fire burned area assessments are carried out using the AWiFS sensor flown on the IRS ResourceSat 1 and 2 satellites for specific fire events.

The northern Indian state of Uttarakhand is richly forested (24,240 sq. km, 45% of the state’s geographical area)¹⁸

and typically exhibits forest fire activity from February to June, with a peak in fire incidence in May and June. During the April 2016 event, forest fires were widespread covering most of the forested regions of the state and the number of fires observed was unusually high. Here we present satellite observations on the event.

Figure 1 shows the spatial distribution of active forest fire detections during 24 April–4 May 2016 in Uttarakhand and Figure 2 shows the temporal occurrence

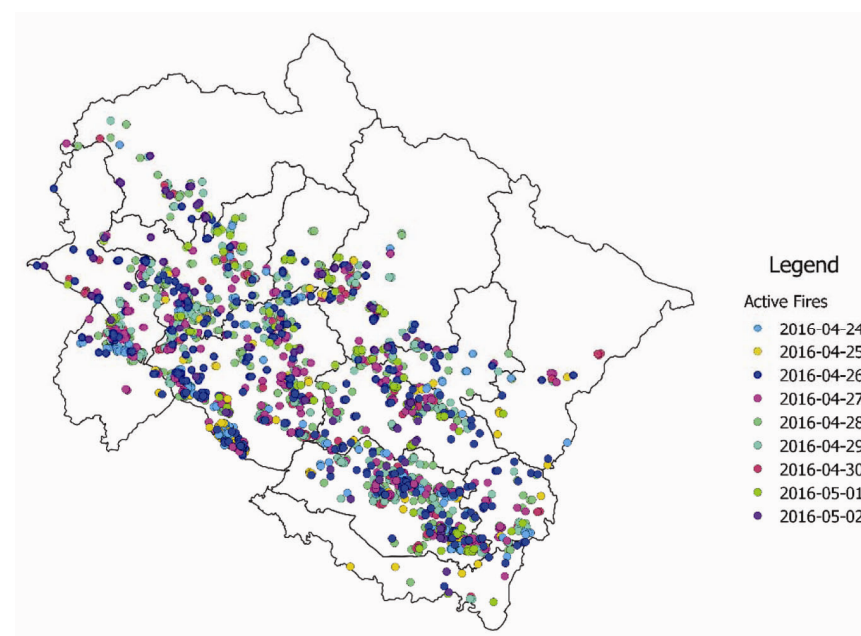


Figure 1. Spatial distribution of cumulative forest fires locations in Uttarakhand, India during 24 April–2 May 2016.

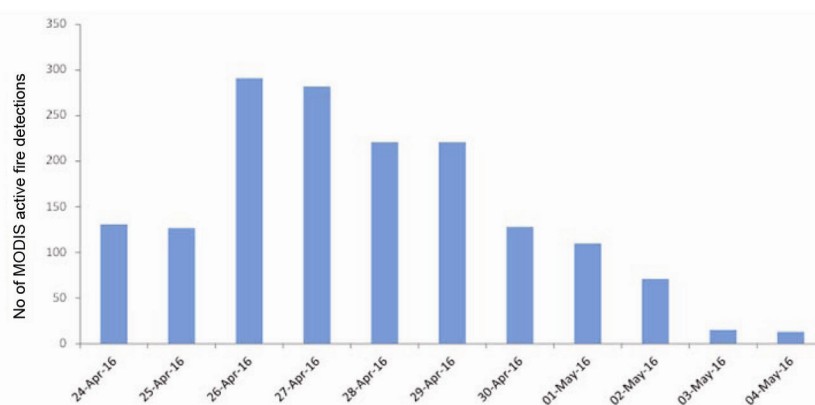
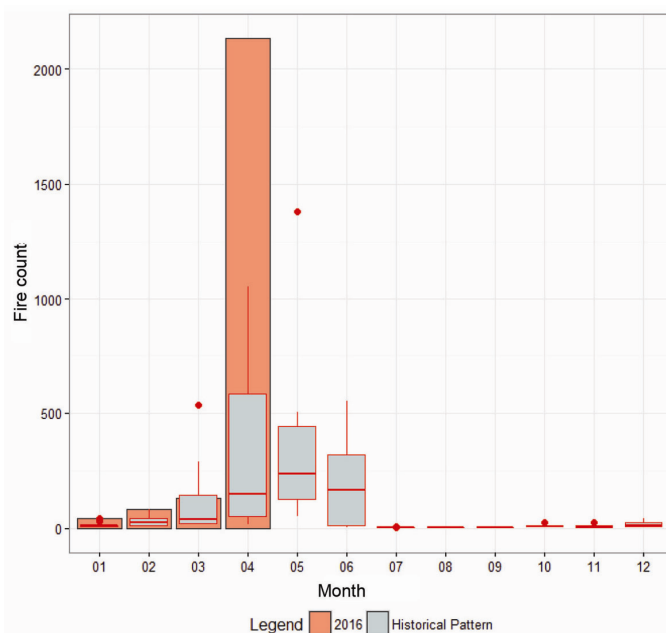


Figure 2. Temporal distribution of forest fires in Uttarakhand from 20 April to 4 May 2016.

of forest fires during the same period. A total of ~1600 active forest fire detections were observed in Uttarakhand during the period. Heightened fire activity started on 24 April 2016, peaked during 26–28 April 2016 and subsequently subsided. The vigorous attempts to contain and control the fires by the State Forest Department and the State administration were aided by rain and persistent cloud and by 2 May 2016, the heightened forest fire activity subsided. The vast majority of forest fires broke out in the Garhwal, Nainital and Almora districts (68%).

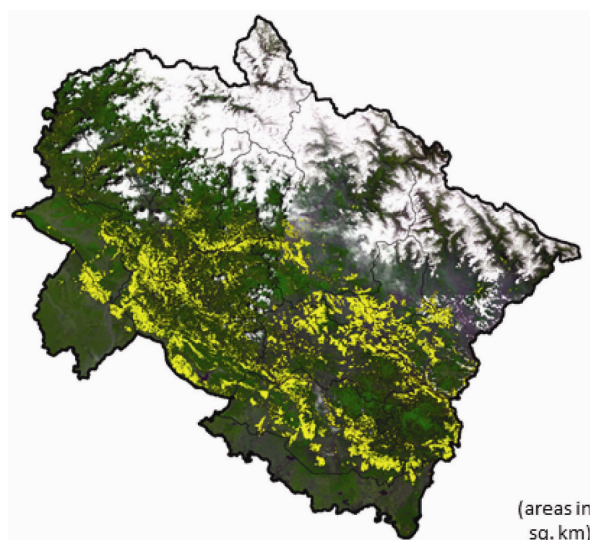
Active fire detections from Terra and Aqua are available from 2003. We compared the month-wise pattern from 2003 to 2015 using AQUA and TERRA MODIS with the 2016 event (Figure 3). The number of active fires detected was highest since 2003. Fires detected in April 2016 were more than twice the previously recorded maximum and nearly five times the 12-yr mean.

Smoke and haze from the fires covered large part of the state. Landsat 8 coverage of 28 April 2016, and AWiFS data from the 3, 4 and 7 May 2016 were used to assess the extent of burned area. Burned areas are visualized by dark black tones in a standard false colour composite – the charcoal signature – because of deposits of soot, charcoal and ash, removal of vegetation, and alteration to the structure of the vegetation. The persistence of this charcoal signature following the burn, is dependent on the dispersal by winds or rain, covering of the deposits by leaf litter or vegetation regrowth. The Modified Burnt Area Index – BAIM¹⁹ – which exaggerates the difference in spectral signature of a pixel to that of charcoal in the SWIR and NIR regions to enable burned area discrimination was used in this study. BAIM values for green season and fire season were calculated. Burned area was discriminated using rule set applied to difference in BAIM values for green season and fire season data²⁰. Burned area mapped with this approach was corrected by visual inspection to avoid commission errors. Terrain shadow, clouds and cloud shadow, and water were masked using in-house developed algorithms. The resulting burned area mask had a low commission rate. The total burned area was estimated to be 2166 sq. km (Figure 4). About 385 sq. km of this area was outside of the forests mapped by FSI¹⁸.



Note: MODIS detections from 2003 to 2015 were used to characterize the historical pattern of forest fires.

Figure 3. Comparison of 2016 fire event with historical pattern.



District	Total geographic area	Forest area	Burned area		Proportion of forest area burned (%)
			Within forest	Outside forest	
Almora	3,139	1,583	149.09	52.28	9.42
Bageshwar	2,246	1,363	212.02	13.62	15.56
Chamoli	8,030	2,681	50.00	14.96	1.87
Champawat	1,766	1,184	79.77	16.74	6.74
Dehra Dun	3,088	1,602	89.90	3.45	5.61
Haridwar	2,360	588	45.67	1.20	7.77
Nainital	4,251	3,004	323.66	18.99	10.77
Pauri Garhwal	5,329	3,269	496.65	105.02	15.19
Pithoragarh	7,090	2,102	201.49	106.50	9.59
Rudraprayag	1,984	1,130	14.93	3.90	1.32
Tehri Garhwal	3,642	2,156	112.75	40.34	5.23
Udham Singh Nagar	2,542	506	4.49	7.44	0.89
Uttarakashi	8,016	3,072			
Total	53,483	24,240	1781.35	384.72	7.35

Figure 4. Burnt area assessment of Uttarakhand and district-wise statistics based on IRS AWiFS multi-temporal datasets.

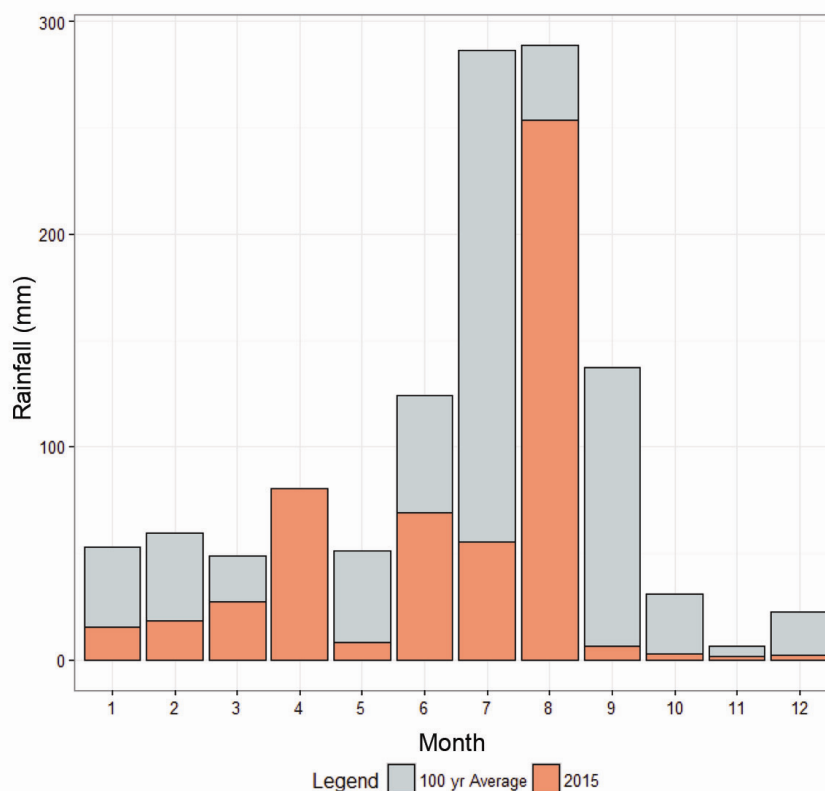


Figure 5. Comparison of 2015 rainfall with 100 years historical average (data source: IMD).

Nearly 87% of the fires occurred in dense forests. The burned area was largely in the moist deciduous (55.29%) and subtropical pine forests (29%), and 7.35% of the forest area of the state was burned in this event. A rapid assessment of the affected districts was carried out after the fires subsided to qualitatively validate the burned area product and collect field observations on the nature of the fires. No commission errors were observed; omissions on account of cloud cover were evident.

We also compared backscatter coefficient (σ_0) values pertaining to HH and HV for burn scars with reference to pre-burn stages in multi-date RISAT-1 C-band MRS Synthetic Aperture Radar (SAR) satellite data (8 April and 3 May 2016). Backscatter coefficient value statistics were collected from training locations that were labelled as burned from the multi-spectral analysis in sal, oak and pine forests. No statistically significant differences in backscatter were detectable, and RISAT-1 C-band MRS data were not found suitable for burned area discrimination in the Uttarakhand episode. The possible explanation for non-detection of burn scars in SAR data

might be due to the reason that most fires were ground-based wherein the crown/canopy is intact, which did not cause any identifiable variability in the image texture. Our field assessment also found the burned area stands intact though scorched. Only two of the locations visited showed signs of canopy fire, while the rest were ground fires that did not involve the upper or middle canopy. Mortality from the fires was exclusively restricted to trees that were debarked very deep for the purpose of resin collection. Resin collection is permitted from trees larger than 120 cm GBH (girth at breast height). Almost all such trees in burned areas showed scorching and injury from fire, while a small proportion of trees had burned through and toppled over. No seedlings/smaller trees (10–30 cm GBH) were observed in the burned areas, suggesting that tree mortality from fires is largely restricted to the smaller girth classes.

Forest fires in India are believed to be exclusively of anthropogenic origin. Discussions during the field visit with residents as well as personnel involved in controlling fires confirm this observation. It is likely that the normal pattern of

fires was amplified by unfavourable climate and a very hot spell. According to India Meteorological Department, the average annual rainfall for the state is 1138 mm, while the annual precipitation was only 47% in 2015, with most of the rainfall occurring in August 2015 (Figure 5).

The present study aims to report the infrastructural as well as advanced technical capabilities of ISRO in addressing forest fires in terms of acquiring, processing and reporting information in near real time. The information includes generation and dissemination of active forest fire alerts in near real time using MODIS and VIIRS data and rapid as well as end-of-season burn area estimates using IRS AWiFS data. Historical active fire information at the national level is also used for fire zonation (forest fire regimes) and are being updated in BHUVAN. The present paper is a case study addressing the recent devastating forest fire episodes that occurred in Uttarakhand and ISRO's role in providing satellite based inputs for fire control and management.

1. Kinnaird, M. F. and O'Brien, T. G., *Conserv. Biol.*, 1998, **12**(5), 954–956.

2. Butry, D. T., Mercer, D. E. and Preston, J. P., *J. For.*, 2001, **99**(11), 9–17.
3. Hao, W. M., Ward, D. W., Olbu, G. and Baker, S. P., *J. Geophys. Res.*, 1996, **101**, 23577–23584.
4. Fearnside, P. M., *Climate Change*, 2000, **46**, 115–158.
5. Crutzen, P. J. and Andreae, M. O., *Science*, 1990, **250**, 1669–1678.
6. Sugihara, N. G., Van Wagtenonk, J. W. and Fites-Kaufman, J., In *Fire in California's Ecosystems*, University of California Press, Berkeley, CA, USA, 2006, pp. 58–74.
7. Gubbi, S., *Deccan Herald*, 2003; <http://wildlifefirst.info/images/wordfiles/fire.doc> (accessed January 2004).
8. FSI, State of the Forest Report, Forest Survey of India, Ministry of Environment and Forests, GoI, 2001.
9. Dwyer, E., Grégoire, J.-M. and Malingreau, J.-P., *Ambio*, 1998, **27**, 175–181.
10. Arino, O. and Rosaz, J., In Proceedings of the Joint Fire Science Conference, 1999, pp. 177–182.
11. Giglio, L., Kendall, J. and Mack, R., *Int. J. Remote Sensing*, 2003, **24**, 4505–4525.
12. Giglio, L., Descloitres, J., Justice, C. O. and Kaufman, Y. J., *Remote Sensing Environ.*, 2003, **87**, 273–282.
13. Prins, E. M., Feltz, J. M., Menzel, W. P. and Ward, D. E., *J. Geophys. Res.: Atmos.*, 1998, **103**, 31821–31835.
14. Calle, A., Casanova, J. and Romo, A., *J. Geophys. Res.: Biogeosci.*, 2006, **111**; <http://dx.doi.org/10.1029/2005JG000116>.
15. Giglio, L., Descloitres, J., Justice, C. O. and Kaufman, Y. J., *Remote Sensing Environ.*, 2003, **87**, 273–282.
16. Csiszar, I. et al., *J. Geophys. Res.: Atmos.*, 2014, **119**, 803–816.
17. Schroeder, W., Oliva, P., Giglio, L. and Csiszar, I. A., *Remote Sensing Environ.*, 2014, **143**, 85–96.
18. FSI, India State of the Forest Report 2015 (WWW document); <http://fsi.nic.in/isfr-2015/isfr-2015-tree-cover.pdf> (accessed on 23 May 2016).
19. Martín, M. P., Gómez, I. and Chuvieco, E., In Proceedings of the 5th International Workshop on Remote Sensing and GIS Applications to Forest Fire Management: Fire Effects Assessment (eds Riva, J., Pérez-Cabello, F. and Chuvieco, E.), Universidad de Zaragoza, Zaragoza, Spain, 2005, pp. 193–198.
20. Singhal, J., Kiran Chand, T. R., Rajashekar, G. and Jha, C. S., ISPRS Technical Commission VIII Symposium, 2014; DOI:10.5194/isprsarchives-XL-8-1429-2014

ACKNOWLEDGEMENTS. This study is being carried out as part of the Decision Support Centre – Disaster Management Support Program (DSC-DMSP) activities of the National Remote Sensing Centre (ISRO), Hyderabad. We thank State Forest Department of

Uttarakhand for providing geospatial inputs and for help during ground validation

Received and accepted 25 May 2016

CHANDRA SHEKHAR JHA*
 RAJASHEKAR GOPALAKRISHNAN
 KIRAN CHAND THUMATY
 JAYANT SINGHAL
 C. SUDHAKAR REDDY
 JYOTI SINGH
 S. VAZEED PASHA
 SURESH MIDDINTI
 MUTYALA PRAVEEN
 ARUL RAJ MURUGAVEL
 S. YUGANDHAR REDDY
 MANI KUMAR VEDANTAM
 ANIL YADAV
 G. SRINIVASA RAO
 GURURAO DIWAKAR PARSII
 VINAY KUMAR DADHWAL

*Forestry and Ecology Group,
 National Remote Sensing Centre (ISRO),
 Balanagar,
 Hyderabad 500 037, India
 *For correspondence.
 e-mail: chandra.s.jha@gmail.com*

Inheritance of andromonoecy in ridge gourd (*Luffa acutangula* Roxb.) L.

Ridge gourd [*Luffa acutangula* (Roxb.) L.], is one of the most important vegetables grown throughout the year in all the tropical regions especially in Asian and African countries. It is rich in vitamin A, C and iron¹. A variety of sex forms, with different genetic mechanisms, were reported in cucurbitaceous crops². Monoecy is governed by a single dominant gene in the monoecious versus andromonoecious sex forms of watermelon and *Cucumis ficifolius*^{3,4}. In contrast, andromonoecy was reported to be controlled by two linked dominant genes in *tibish* group of melon⁵. Also, the digenic nature of inheritance of monoecious, andromonoecious, gynomoecious/gynoecious and hermaphrodite conditions showing F₂ ratio of 9 : 3 : 3 : 1 was reported in *Cucumis melo*⁶ and *Luffa acutangula*^{7,8}.

In the ridge gourd germplasm, IIHR-43 (IC110893) maintained in the laboratory at ICAR-IIHR, an andromonoecious plant which bore male and hermaphrodite flowers on the same plant was noticed during 2010. This variant was designated as 'Andromon-43' (AM-43). It was found to breed genetically true to type in subsequent generations of selfing, but produced short fruits.

Observations on morphological traits of AM-43 and the normal monoecious types are presented in Table 1. It is interesting to note that the AM-43 was accompanied by certain features, but phenotypically distinct from the monoecious lines. The observations revealed that flowering in AM-43 was early and the first female flower emerged at lower nodes (5.9) compared to monoecious

(9.5–13.9 node). Further, AM-43 produced very small leaves (179.1 cm² versus 311.6–370.2 cm²), an oval and short ovary (Figure 1d) and well-developed anthers encircling the stigma (Figure 1c). AM-43 produced a larger number of fruits/plant (52.4) compared to monoecious types (5.4–10.6). However fruits developing on AM-43 were extremely short (5.4 cm versus 30.1–45.2 cm; Figure 1f and g).

To understand the inheritance of andromonoecy in ridge gourd, crosses were effected during 2012 monsoon. The andromonoecious line, AM-43 was crossed as male parent with three normal monoecious lines, viz. IIHR-6, IIHR-70 and IIHR-73. A total of 24 F₀ seeds from well-developed fruits were extracted to raise F₁ generation of each cross in the